Compatibility, Morphology, and Crystallization Behavior of Compatibilized β-Nucleated Polypropylene/ Poly(trimethylene terephthalate) Blends

Zhidan Lin, Chao Chen, Baicheng Li, Zixian Guan, Zhuoyao Huang, Meng Zhang, Xue Li, Xiuju Zhang

College of Science and Engineering, Jinan University, Guangzhou 510632, People's Republic of China

Received 28 June 2011; accepted 12 September 2011
DOI 10.1002/app.35635
Published online 16 January 2012 in Wiley Online Library (wileyonlinelibrary.com).

ABSTRACT: β-Nucleated polypropylene (PP), uncompatibilized β-nucleated PP/poly(trimethylene terephthalate) (PTT), β-nucleated PP/PTT blends compatibilized with maleic anhydride (MA)-grafted PP (PP-*g*-MA), and styrene–ethylene–propylene copolymer were prepared with a twin-screw extruder. The morphology, compatibility, crystallization characteristic, melting behavior, and crystallization kinetics were investigated. The result shows that β-nucleated PP was incompatible with PTT, and the addition of the two compatibilizers decreased the interfacial tension between β-nucleated PP and PTT; this led to improved dispersion and strengthened interfacial bonding in the blends. PP-*g*-MA had a better compatibilization effect. All of the researched β-nucleated PP/PTT blends contained β crystals of PP, and the compatibilizers exhibited synergistic effects with the β-nucleating agent to further increase the content of β crystals. Nonisothermal kinetic analysis indicated that Mo's method described the nonisothermal crystallization behavior of the β-nucleated PP/PTT blends satisfactorily, and the Avrami approach could only describe the early stage of the crystallization appropriately, whereas the Ozawa method failed to have the same effect. © 2012 Wiley Periodicals, Inc. J Appl Polym Sci 125: 1616–1624, 2012

Key words: blends; compatibilization; crystallization; morphology; poly(propylene) (PP)

INTRODUCTION

Isotactic polypropylene (PP) is one of the most versatile common thermoplastic polymers because of its outstanding performance; its properties include an excellent chemical resistance, water resistance, good ductility, and low processing costs. Moreover, isotactic PP is a kind of polymorphic material with three known potential crystals, namely, α, β, and γ crystals.[1] Recently, more attention has been paid to the β crystal because of its excellent thermal and mechanical properties, such as a higher heat distortion temperature and an improved elongation at break and impact strength.[2–4] From the perspective of industrial applications, these features are very important. However, because of its worse stability compared to that of α-nucleated PP (α-PP), a high β-crystal content (K_β) can only be obtained under certain crystallization conditions, such as the addition of a β-nucleating agent,[5] shearing melting,[6] and temperature gradient.[7] Moreover, the yield strength and elastic modulus of β-nucleated PP (β-PP) were lower than those of α-PP. To improve the performance of β-PP, the blending β-PP with other polymers will be an increasingly important method.

Feng et al.[8] observed that during the process of cavity filling, the shear flow field significantly affected the formation of β-PP in the blends of PP and the nylon 6/clay nanocomposites. Under the appropriate crystallization conditions of the molding process, the high shear between the nylon 6/clay phase and PP matrix could induce the formation of β-PP. They also found that in the injection molding process, it was the nylon 6/clay phase rather than nylon 6 that obviously induced the formation of β-PP. However, a better understanding of the formation mechanism in the process is needed. It was also observed that while being compounded with amorphous compounds such as the elastomers,[9] β-PP could be easily prepared. Moreover, an important factor in the formation of β-PP in the blends was the crystallization temperature of the second component with α-nucleation.[10] If the second component with α-nucleation had a crystallization temperature lower than that of pure PP, it did not affect the formation of β-PP. On the contrary, if the second component with α-nucleation had a higher crystallization temperature than that of pure PP, the formation of β-PP was inhibited.[10] For

Correspondence to: Z. Lin (linzd@jnu.edu.cn).

Contract grant sponsor: Fundamental Research Funds for the Central Universities of China; contract grant number: 21609711.

Contract grant sponsor: Technology Funds of Guangdong Province of China; contract grant number: 2010A080804021.

Contract grant sponsor: National Natural Science Funds of China; contract grant number: 21101076.

example, in the β-nucleated PP/Polyvinylidene fluoride (PVDF) blend and the β-nucleated PP/nylon 6 (PA6) blend, β-PP could not be formed, even in the presence of a highly effective β-nucleating agent because of the strong β-nucleating ability and the higher crystallization temperature of PVDF and PA6.

Yang et al.[11–13] observed that in β-nucleated PP/PA6 blends, K_β increased with decreasing content of PA6. However, in β-nucleated PP/PA6 blends modified by a PP-*g*-maleic anhydride (MA) compatibilizer, a high K_β could be obtained, and it was not influenced by the PA6 content. This was obviously due to the fact that the PP-*g*-MA could encapsulate PA6; this interfered with the nucleation effect of PA6 on PP. Menyhárd et al.[14] also observed that the formation of a β-PP matrix in β-nucleated PP/PA6 without a compatibilizer was related to the selective encapsulation of a β-nucleating agent in the polar PA6 phase, whereas the addition of PP-*g*-MA improved the distribution of the β-nucleating agent in the PP phase to form a matrix rich in β crystals. Yang and Mai[15] also studied ethylene vinyl acetate copolymer (EVA)-*g*-MA crystallization behavior and the melting characteristics and K_β of β-nucleated PP/PA6. They confirmed that during the compounding process at high temperatures, the nucleating agent was mainly distributed in the PA6 phase and the interfacial phase between PP and PA6.

However, this research focused on the blends of β-nucleated PP with some polar polymers and their modification by polar compatibilizers. Poly(trimethylene terephthalate) (PTT) is a new kind of crystalline polyester, and its blends with some polyolefins, such as PP,[16] PE,[17] and PS,[18] have been reported. However, there has been no report on the blends of PTT with β-nucleated PP. In this study, we adopted a β-nucleated PP/PTT incompatible blend system as the research object and investigated the effect of two compatibilizers with different compatibilization mechanisms on the morphology, compatibility, crystallization behavior, melting characteristics, and crystallization kinetics of the β-nucleated PP/PTT blends to obtain an in-depth understanding of this new promising material.

EXPERIMENTAL

Materials

Isotactic PP (HP500N, MFR 12) was supplied by Reliance Industries, Ltd. (Mumbai, India). PTT was supplied in pellet form by Shell Chemicals (Calgary, Canada), and the trade name was Corterra Polymer 9200. The melting temperature (T_m) was 228°C, and the intrinsic viscosity of the PTT pellet was 0.92 dL/g. Styrene–ethylene–propylene block copolymer (SEP; SEPTON1001, styrene content = 35%) was purchased from Kuraray, Inc (Shanghai, China). PP-*g*-MA (containing 1.0 wt % MA) was supplied by Guangzhou Lushan Chemical Materials Co., Ltd. (Guangzhou, China). A commercial β-nucleating agent, named TMB5, with the chemical component of *N,N′*-dicyclohexylterephthalamide was obtained from Shanxi Provincial Institute of Chemical Industry (Shanxi, China). Glycol reagent (above 99.0% glycol mass fraction content) was provided by Tianjing Fuyu Fine Chemicals Co., Ltd. (Tianjing, China).

Preparation of the composites and test specimens

First, PP and TMB-5 with a mass ratio of 0.4/100 were mixed and blended with a twin-screw extruder (Nanjing Jieya Extrusion Equipment Company, Nanjing, China) at temperatures of 170–200°C to prepare the β-nucleated PP. Then, β-nucleated PP was mixed with PTT and the compatibilizers, whose volume ratio was 70/30/5. Finally, the mixtures were blended with the twin-screw extruder at temperatures of 200–250°C to prepare the compatibilized β-nucleated PP/PTT blends. In comparison, β-nucleated PP/PTT blends with a volume ratio of 70/30 were also prepared under the same conditions. All of the blends were molded in an injection-molding machine (Haitian Plastic Machinery Company, Guangdong, China) at 250°C to obtain impact specimens for scanning electron microscopy (SEM) testing.

Differential scanning calorimetry (DSC) characterization

A TA Instruments Q200 differential scanning calorimeter (TA instrument company, America) was used to study the thermal behavior of the β-nucleated PP/PTT blends, and T_m of the pure indium was used as the calibration standard. A sample of about 5 mg was accurately weighed for DSC testing, and all measurements were performed in a nitrogen atmosphere.

In nonisothermal crystallization and melting behavior characterization, a sample of the blends was heated to 260°C at the rate of 100°C/min and then held for 3 min. Subsequently, it was cooled to 60°C at a cooling rate of 10°C/min for the crystallization behavior study. Then, it was reheated to 260°C at 10°C/min for the melting behavior study.

In the nonisothermal crystallization kinetic study, the sample of the blends was rapidly heated to 200°C and then held for 2 min. Subsequently, it was cooled to 60°C at selected cooling rates ranging from 5 to 40°C/min. Each sample was used only once.

Wide-angle X-ray diffraction (WAXD) analysis

The X-ray diffraction experiment was conducted with the injection-molding sample with a Rigaku Geigerflex model D/Max-III A rotating anode X-ray

diffractometer (Rigaku Corporation, Japan). Graphite monochromatic Cu Kα radiation was used as the radiation source. The scanning range was 5–40° with a rate of 4°/min and a step length of 0.02. K_β was determined according to the standard procedure described in the literature.[19] The formula was as follows:

$$K_\beta = \frac{H_{\beta(300)}}{H_{\beta(300)} + H_{\alpha(110)} + H_{\alpha(040)} + H_{\alpha(130)}} \quad (1)$$

where $H_{\Omega(hkl)}$ denotes the intensity of the respective (hkl) peak belonging to phase Ω.

Morphology observation

The impact specimens were broken according to the impact property test conditions. The fracture surface of the specimens were sputter-coated with gold before the SEM analysis was conducted. The fracture surface morphology of the composites was observed on a Philips XL-30 environmental scanning electron microscopy (ESEM) microscope (Dutch Royal Philips Electronics Company, Amsterdam, Netherlands) with an acceleration voltage of 15 kV.

Contact angle (θ) measurement and surface tension (γ) calculation

The θ values of two test liquids (water and glycerin) of the β-nucleated PP/PTT blends were measured by a sessile drop method at 25°C with a Germanic optical θ tester DSA100 (Kruss Optronic Company, Hamburg, Germany). The sessile drop was formed by the deposition of the liquid with a manual microsyringe on the glossy blend surface. Both the left and the right θ values and the drop dimension parameters were automatically calculated from the digital images. The θ values for both sides of each drop were measured as a function of time intervals of 5 s when instant contact was made between the liquid and the substrate. The measurements were the average of at least five θ values.

γ and its dispersive component (γ^d) and polar component (γ^p) of the β-nucleated PP/PTT blends were calculated on the basis of the harmonic-mean equations[20] as follows:

$$(1 + \cos\theta_{1s})\gamma_1 = 4\left[\frac{\gamma_1^d\gamma_s^d}{\gamma_1^d + \gamma_s^d} + \frac{\gamma_1^p\gamma_s^p}{\gamma_1^p + \gamma_s^p}\right] \quad (2)$$

$$(1 + \cos\theta_{2s})\gamma_2 = 4\left[\frac{\gamma_2^d\gamma_s^d}{\gamma_2^d + \gamma_s^d} + \frac{\gamma_2^p\gamma_s^p}{\gamma_2^p + \gamma_s^p}\right] \quad (3)$$

$$\gamma_s = \gamma_s^d + \gamma_s^p \quad (4)$$

where the subscripts 1, 2, and s correspond to the two kinds of the liquids being tested and the polymer material, respectively, and θ_{1s} and θ_{2s} are the contact angles of each liquid being tested and the polymer material, respectively.

Calculation of the work of adhesion and interfacial tension

The compatibility of the blends could be studied through the interfacial tension and the work of adhesion. The work of adhesion and the interfacial tension of the β-nucleated PP/PTT blends were calculated from γ^d and γ^p of the blend components with the following equations:[20]

$$W_{12} = 4\left[\frac{\gamma_1^d\gamma_2^d}{\gamma_1^d + \gamma_2^d} + \frac{\gamma_1^p\gamma_2^p}{\gamma_1^p + \gamma_2^p}\right] \quad (5)$$

$$\gamma_{12} = \gamma_1 + \gamma_2 - W_{12} \quad (6)$$

where W is the work of adhesion and the subscripts 1 and 2 correspond to the two blend components: $\gamma_1 = \gamma_1^d + \gamma_1^p$ and $\gamma_2 = \gamma_2^d + \gamma_2^p$.

Nonisothermal crystallization kinetics theoretical background

The relative crystallinity at different crystallization times (X_c) could be calculated according to the following equation:[21]

$$X_c = \int_{T_0}^{T} \frac{dH(T)}{dT} dT \Big/ \int_{T_0}^{T_\infty} \frac{dH(T)}{dT} \quad (7)$$

where T_0 and T_∞ are the onset and end crystallization temperatures, respectively, and $dH(T)/dT$ is the rate of heat evolution at temperature T.

The Avrami equation[22] has been widely used to study the nonisothermal crystallization kinetics of polymer, and its equation is as follows:

$$1 - X(t) = \exp(-Z_t^n) \quad (8)$$

where $X(t)$ is the relative crystallinity at time t, n is the Avrami index, and Z_t is a constant related to the crystallization growth and nucleation. Time t could be obtained from the following equation:

$$t = |T_0 - T|/\phi \quad (9)$$

where ϕ is the cooling rate. Therefore, the relationship between X_c and t could be determined.

Ozawa[23,24] took the crystallization growth and nucleation into account and further expanded the Avrami equation to investigate the heating and cooling processes at a constant cooling rate. The double-logarithm form of the Ozawa equation is as follows:

$$\ln[-\ln[1 - X(T)]] = \ln K(T) - m\ln\phi \quad (10)$$

where $X(T)$ is the relative crystallinity at temperature T; $K(T)$ is a function related to the decline of the

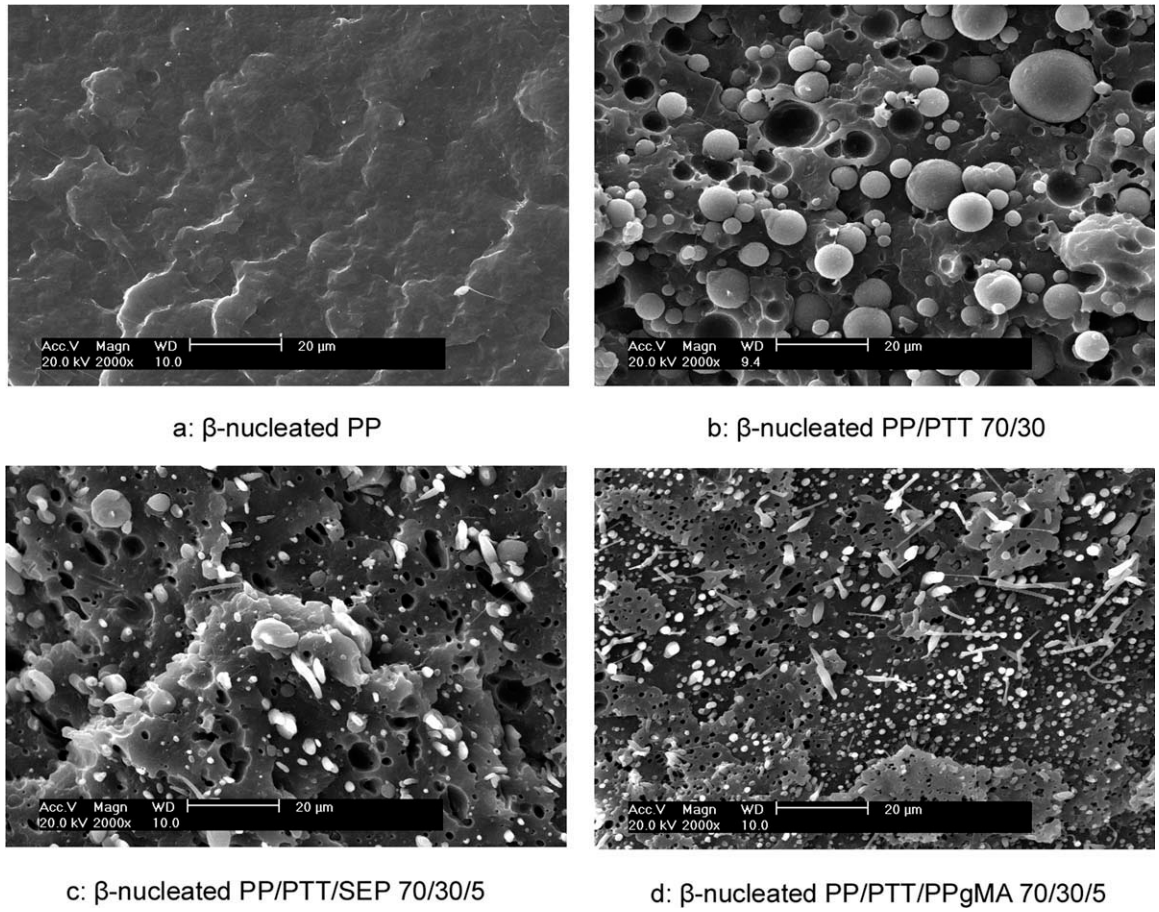

Figure 1 SEM pictures of the fracture surfaces of the β-nucleated PP, uncompatibilized β-nucleated PP/PTT blend, and β-nucleated PP/PTT blends compatibilized with SEP and PP-*g*-MA.

crystallization rate, namely, the speed of crystallization; m is the Ozawa index similar to Avrami index and responds to the crystallization growth and nucleation; and ϕ is the cooling rate.

Mo et al.[25,26] combined the Avrami and Ozawa equations; this led to the ϕ–t model for nonisothermal crystallization as follows:

$$\ln \phi = \ln F(T) - \alpha \ln t \tag{11}$$

where $F(T) = [K(T)/Z_t]^{\frac{1}{m}}$, $\alpha = n/m$, and ϕ is the cooling rate. The physical meaning of $F(T)$ is the required cooling rate at which the system reaches a certain degree of crystallinity in unit time. It represents the level of ease where the sample reaches a certain degree of crystallinity in a given time.

Moreover, Kissinger[27] suggested a method to determine the activation energy for the transportation of the macromolecular segments to the growing surface (ΔE) by calculating the variation of the peak temperature of crystallization (T_p) with the cooling rate (ϕ):

$$\frac{d[\ln(\phi/T_p^2)]}{d(1/T_p)} = -\frac{\Delta E}{R} \tag{12}$$

where R is the gas constant and ΔE is calculated from the slope of a plot of $\ln(\phi/T_p^2)$ versus $1/T_p$.

RESULTS AND DISCUSSION

Morphology

Figure 1 shows the SEM micrographs of the fracture surface of the β-nucleated PP, uncompatibilized β-nucleated PP/PTT blends, and β-nucleated PP/PTT blends compatibilized with SEP and PP-*g*-MA. The fracture surface of β-nucleated PP [see Fig. 1(a)], on which the small white particles were observed, was smooth. These particles were the β-nucleating agent TMB-5, which would not melt during the compounding process. On the fracture surface of the uncompatibilized β-nucleated PP/PTT blends [see Fig. 1(b)], the dispersed phase, with a particle size between 5 and 12 μm, of the spherical PTT could be observed, and an obvious interface existed between the PTT phase and the β-nucleated PP phase. This showed poor interfacial bonding between PP and PTT, so it was necessary to improve the compatibility of their blends with the compatibilizer. Compared with the uncompatibilized blends, the particle

TABLE I
γ Values of the β-Nucleated PP/PTT Blends Calculated According to Harmonic-Mean Equations

Sample	β-Nucleated PP		PTT		β-Nucleated PP/PP-*g*-MA		β-Nucleated PP/SEP	
Test liquid	Water	Glycol	Water	Glycol	Water	Glycol	Water	Glycol
θ (°)	105.0	77.7	87.0	58.8	100.9	77.0	105.0	85.0
γ (mN/m)	21.5		29.6		22.8		18.4	
γ^d (mN/m)	14.7		18.3		19.1		8.6	
γ^p (mN/m)	6.8		11.2		3.7		9.8	

size of the PTT dispersed phase was smaller, and the particle distribution was more uniform on the fracture surface of the β-nucleated PP/PTT blends compatibilized with SEP [see Fig. 1(c)]. The PTT phase and the β-nucleated PP phase bonded tightly, and the exposed particles also had signs of being stretched. This may have been due to the fact that SEP had a similar chain structure to the β-nucleated PP and PTT; this reduced the interfacial energy between them and promoted good dispersion and a uniform distribution of the PTT phase. Therefore, SEP had an effective compatibilization effect on the β-nucleated PP/PTT blending system. Compared with the blend modified by SEP, the particle size of the PTT phase decreased further to 1 μm, and the particle distribution was more uniform on the fracture surface of the β-nucleated PP/PTT blends compatibilized with PP-*g*-MA [see Fig. 1(d)]. The fracture surface of the blends was smooth, and the interfacial bonding between the PTT phase and the PP phase was tight. This may have been due to the fact that the MA group of PP-*g*-MA could react with the hydroxyl group of PTT;[16] this led to much better interfacial bonding. Hence, PP-*g*-MA was more favorable for the promotion of the compatibility of PP and PTT.

Compatibility analysis

The compatibility of the polymer blends could be studied through the measurement of interfacial tension and the work of adhesion of the blends. To study the compatibility in the compatibilized β-nucleated PP/PTT blends, the β-nucleated PP/SEP blends and β-nucleated PP/PP-*g*-MA blends were also prepared by the same process. The pure water and glycol were taken as liquids to be tested. The γ, γ^d, and γ^p values of pure water[28] and glycol[29] were 72.8, 21.8, and 51 and 47.2, 29.7, and 17.5 mN/m, respectively. The θ values of the tested liquids to the

TABLE II
Interfacial Tension and Work of Adhesion of the β-Nucleated PP, β-Nucleated PP/SEP Blend, and β-Nucleated/PP-*g*-MA Blend with PTT

Matrix	β-Nucleated PP	β-Nucleated PP/SEP blend	β-Nucleated PP/PP-*g*-MA blend
Dispersed phase		PTT	
γ (mN/m)	2.0	1.8	0.8
W (mN/m)	50.3	46.1	50.3

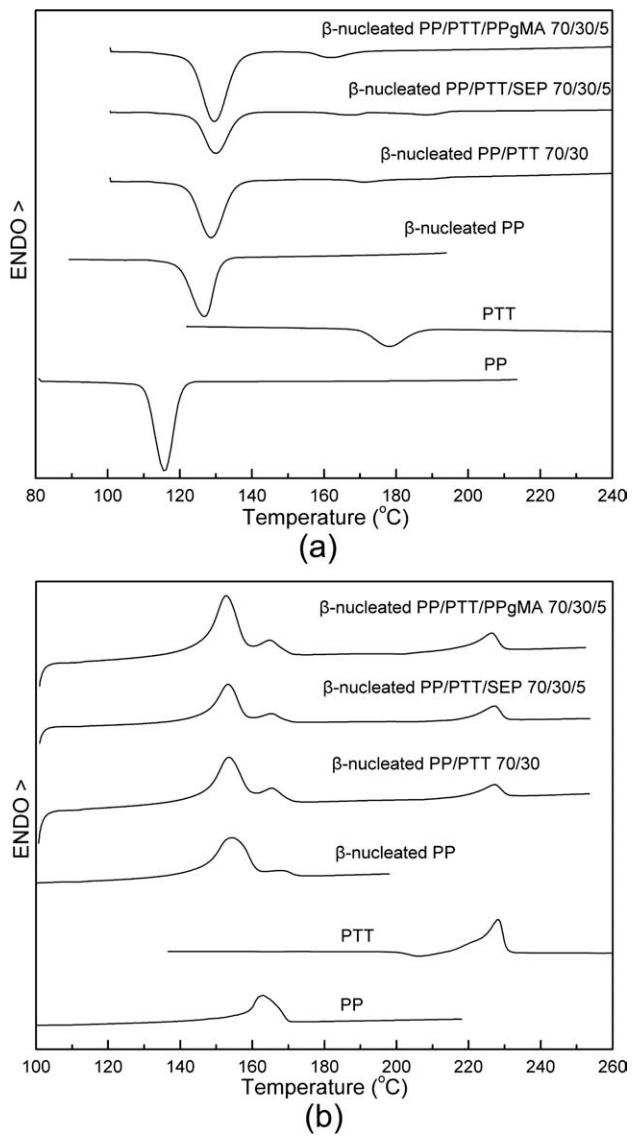

Figure 2 (a) Crystallization and (b) melting curves of the β-nucleated PP, uncompatibilized β-nucleated PP/PTT blend, and β-nucleated PP/PTT blends compatibilized with SEP and PP-*g*-MA.

TABLE III
Nonisothermal Crystallization and Melting Parameters of the PP, β-Nucleated PP, β-Nucleated PP/PTT Blend, and β-Nucleated PP/PTT Blend Compatibilized with SEP and PP-*g*-MA

Sample	PP phase					PTT phase				
	T_c^p (°C)	ΔH_c (J/g)	$T_m^p(\beta)$ (°C)	$T_m^p(\alpha)$ (°C)	ΔH_m (J/g)	T_c^p 1 (°C)	T_c^p 2 (°C)	ΔH_c (J/g)	T_m^p (°C)	ΔH_m (J/g)
PP	115.4	95.8	—	162.8	96.9	—	—	—	—	—
β-PP	126.9	83.9	154.2	167.8	92.5	—	—	—	—	—
PTT	—	—	—	—	—	—	181.4	51.7	227.8	63.5
β-PP/PTT	128.7	63.6	153.4	165.9	71.8	171.6	190.0	7.0	227.2	10.3
β-PP/PTT/SEP	130.1	59.5	153.2	165.7	66.1	167.2	188.3	13.0	227.1	14.9
β-PP/PTT/PPgMA	129.6	69.6	152.7	165.3	74.1	162.5	—	5.9	226.4	14.5

blends are listed in Table I. Therefore, the γ, γ^d, and γ^p values of each material were calculated according to eqs. (2) and (3) and are also shown in Table I. The interfacial tension and the work of adhesion of PTT to β-nucleated PP, β-nucleated PP/SEP, and β-nucleated PP/PP-*g*-MA calculated according to eqs. (4) and (5) and are shows in Table II. It can be seen that the addition of compatibilizer SEP decreased the interfacial tension between the β-nucleated PP phase and the PTT phase. Compared with SEP, PP-*g*-MA further decreased the interfacial tension and increased the work of adhesion between the β-nucleated PP phase and the PTT phase. The smaller interfacial tension and higher work of adhesion indicated better interfacial bonding. Therefore, both SEP and PP-*g*-MA enhanced the interfacial compatibility of the β-nucleated PP/PTT blends, and PP-*g*-MA had the better effect. This was consistent with the results of SEM observation.

Nonisothermal crystallization and melting behavior characterization

Figure 2 shows the DSC crystallization and melting curves of the β-nucleated PP, uncompatibilized β-nucleated PP/PTT blends, and β-nucleated PP/PTT blends compatibilized with SEP and PP-*g*-MA, and the corresponding data are listed in Table III. It can be seen that the crystallization peak temperature (T_c^p) of β-nucleated PP with TMB-5 increased from 115.4°C for pure PP to 126.9°C, and its melting curve also changed from a single peak of pure PP to double melting peaks. The low-temperature melting peak corresponded to the β-crystal melting process of PP, whereas the high-temperature melting peak corresponded to the α-crystal melting process. The height of low-temperature melting peak was higher than that of the high-temperature melting peak. In addition, both the crystallization enthalpy (ΔH_c) and the melting enthalpy (ΔH_m) of the β-nucleated PP were lower than those of pure PP; this was in accordance with a report[1] that indicated that the enthalpy of the β crystals was lower than that of the α crystals. Thus, TMB-5 was an effective β-nucleating agent. In the uncompatibilized β-nucleated PP/PTT blends, T_c^p of the PP phase increased, and ΔH_c decreased with the addition of PTT. This indicated that the PTT phase had a nucleation effect on PP crystallization. The double melting peaks also appeared on the melting curve; however, the low-temperature melting peak temperature and high-temperature melting peak temperature were both lower than those of the β-nucleated PP. This may have been due to the fact that the addition of PTT led to the reduction of crystal perfection and thinned crystal thickness. Compared with the uncompatibilized β-nucleated PP/PTT blends, the crystallization peak temperature (T_c^p) and melting peak temperature (T_m^p) of the PP phase in the β-nucleated PP/PTT blends compatibilized with SEP and PP-*g*-MA

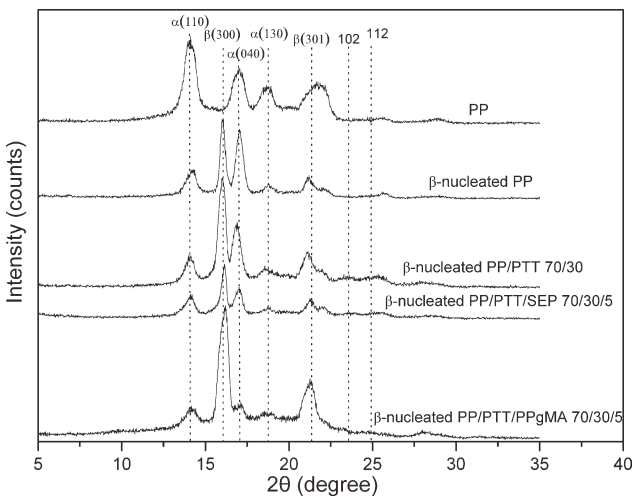

Figure 3 WAXD patterns of the β-nucleated PP, uncompatibilized β-nucleated PP/PTT blend, and β-nucleated PP/PTT blends compatibilized with SEP and PP-*g*-MA.

TABLE IV
K_β Values for the PP, β-Nucleated PP, β-Nucleated PP/PTT Blend, and β-Nucleated PP/PTT Blend Compatibilized with SEP and PP-*g*-MA

Sample	PP	βPP	βPP/PTT	βPP/PTT/SEP	βPP/PTT/PP-*g*-MA
K_β	0	0.41	0.44	0.45	0.57

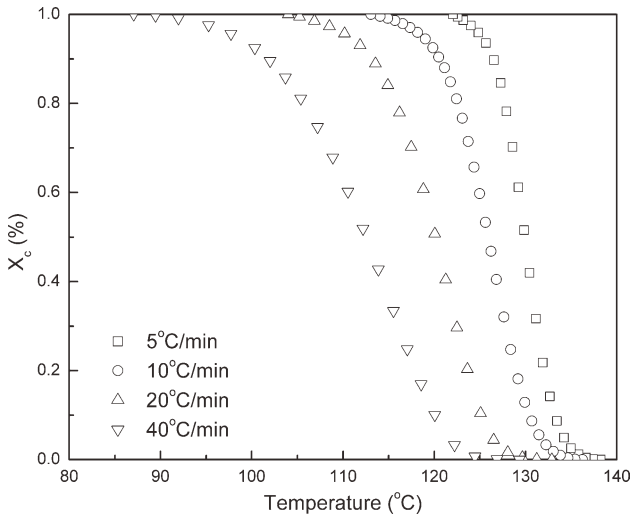

Figure 4 Nonisothermal crystallization kinetic curves of X_c versus T.

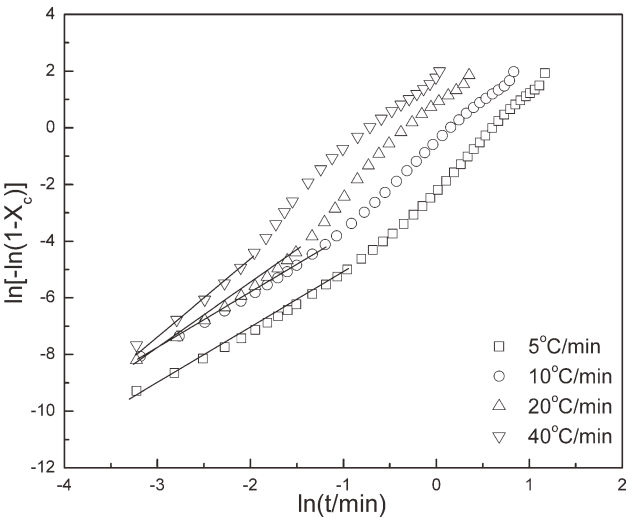

Figure 6 Nonisothermal crystallization kinetic curves of $\ln[-\ln(1 - X_c)]$ versus $\ln t$ according to the Avrami equation.

changed little. However, for the PTT crystal, when the content of PTT was 30 vol %, the crystallization behavior of the PTT phase changed significantly. T_c^p of PTT differentiated into two peaks at 171.6 and 190.0°C. The low-temperature peak of the PTT may have been related to the fractionalized crystallization behavior of PTT. When one polymer is dispersed into another polymer with low T_m into small droplets, its crystallization temperature can be largely decreased.[30] The high-temperature peak may have been related to the nucleation effect of the β-nucleating agent TM5 to PTT. With the addition of the SEP, double crystallizing peaks still emerged in PTT, and both of the peak temperatures decreased. This indicated that SEP increased the compatibility of the blends and strengthened the fractionalized crystallization behavior of PTT. However, SEP also decreased the transferring quantity of TM5 into the PTT phase and weakened the nucleation effect to PTT. With the addition of PP-*g*-MA, the crystallization curve of PTT changed to a single peak. This may have been due to the fact that the polar PP-*g*-MA increased the compatibility of the blends and might have completely stopped the transference of TM5 into the PTT phase.[11–13] Moreover, the fractionalized crystallization behavior of PTT was greatly strengthened, which decreased T_c^p to 152.5°C. This suggested that the addition of PP-*g*-MA greatly improved the compatibility of PTT and PP; this was in accordance with the results of SEM observation.

Figure 3 presents the WAXD patterns of the β-nucleated PP, uncompatibilized β-nucleated PP/PTT blends, and β-nucleated PP/PTT blends compatibilized with SEP and PP-*g*-MA. Table IV shows the K_β

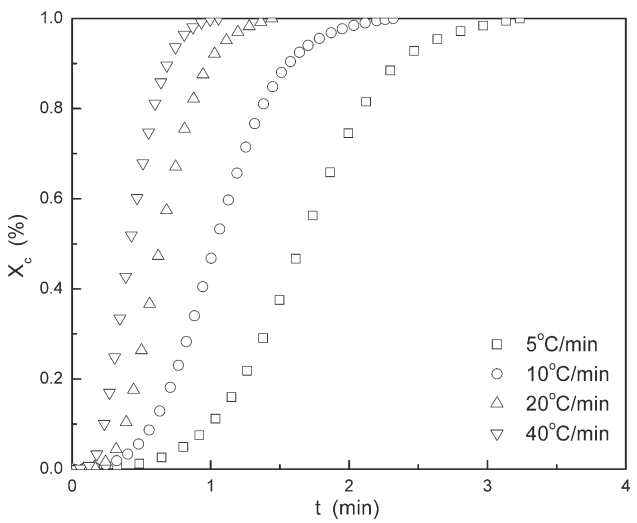

Figure 5 Nonisothermal crystallization kinetic curves of X_c versus time.

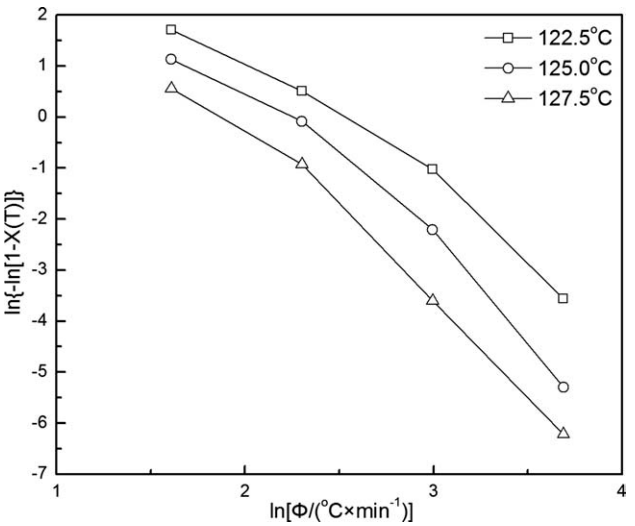

Figure 7 Nonisothermal crystallization kinetic curves of $\ln\{-\ln[1 - X(t)]\}$ versus $\ln \phi$ according to Ozawa method.

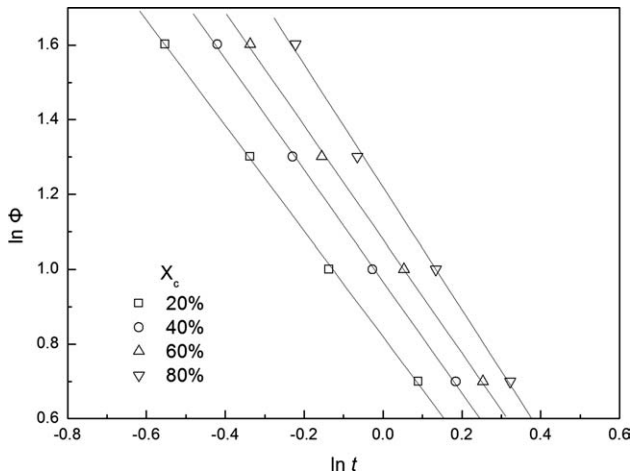

Figure 8 Nonisothermal crystallization kinetic curves of log ϕ versus ln t according to the Mo method.

values calculated according to eq. (1). The K_β value of pure PP was close to zero. The K_β value of the uncompatibilized β-nucleated PP/PTT blends was 0.41; this indicated that TMB-5 was an effective β-nucleating agent. Compared with the uncompatibilized β-nucleated PP/PTT blends, the K_β value of the blends compatibilized with SEP changed slightly. However, the K_β value of the β-nucleated PP/PTT blends compatibilized with PP-*g*-MA increased markedly. This may have been attributed to the fact that PP-*g*-MA had a better compatibilization effect than SEP and promoted the dispersion of the β-nucleating agent. Therefore, the preparation method of this study achieved high K_β in the PP/PTT blends.

Crystallization kinetics

X_c could be obtained at any crystallization temperature (T), as is shown in Figure 4, for the β-nucleated PP/PTT blends. It can be seen that with increasing cooling rate, the crystallization temperature shifted toward a lower temperature. For the nonisothermal crystallization process at a constant cooling rate, the curve of X_c versus T could be transferred into the curve of X_c versus time t (as shown in Fig. 5). It can be seen that with the increase of the cooling rate, the crystallization time decreased. The Avrami curves of the β-nucleated PP/PTT blends showed poor linearity at the later stage (see Fig. 6); this suggested that the Avrami equation was not very suitable for analyzing the later stage of the nonisothermal crystallization kinetics of the β-nucleated PP/PTT blends in this study. From $X(t)$ versus ln ϕ according to the Ozawa method (see Fig. 7), it can be seen that the curves showed poor linearity in the whole process; this indicated that the Ozawa method failed to describe the nonisothermal crystallization kinetics of the β-nucleated PP/PTT blends in this study. The curves of ln ϕ versus ln t for the β-nucleated PP/PTT blends based on the Mo method are shown in Figure 8. It can be seen that the linearity was good; this indicated that the Mo method was adequate to describe the nonisothermal crystallization process of the β-nucleated PP/PTT blends in this study. The α and $F(T)$ values of all of the β-nucleated PP/PTT blends based on the Mo method are listed in Table V. The values of $F(T)$ systematically increased with increasing X_c of all of the β-nucleated PP/PTT blends. This indicated that a higher crystallization

TABLE V
Nonisothermal Crystallization Kinetic Parameters of the β-Nucleated PP, Uncompatibilized β-Nucleated PP/PTT Blend, and β-Nucleated PP/PTT Blends Compatibilized with SEP and PP-*g*-MA

Sample	X_c (%)	α	$F(T)$ (K/min^{a-1})	Φ (°C/min)	T_p (°C)	ΔE (kJ/mol)
α-PP	20	1.3	2.3	5	119.7	171.1
	40	1.3	2.6	10	115.5	
	60	1.4	2.8	20	111.7	
	80	1.5	3.1	40	103.8	
β-Nucleated PP	20	1.4	2.2	5	130.5	243.3
	40	1.5	2.4	10	126.8	
	60	1.6	2.7	20	123.4	
	80	1.7	3.1	40	118.8	
β-Nucleated PP/PTT 70/30	20	1.4	2.3	5	130.1	181.5
	40	1.5	2.6	10	126.3	
	60	1.5	2.9	20	121.6	
	80	1.6	3.4	40	114.8	
β-nucleated PP/PTT/SEP 70/30/5	20	1.5	2.4	5	131.0	237.0
	40	1.5	2.7	10	127.8	
	60	1.5	2.9	20	123.6	
	80	1.6	3.3	40	119.2	
β-Nucleated PP/PTT/PP-*g*-MA 70/30/5	20	1.3	2.3	5	131.2	237.7
	40	1.4	2.6	10	127.6	
	60	1.4	2.9	20	123.8	
	80	1.5	3.2	40	119.4	

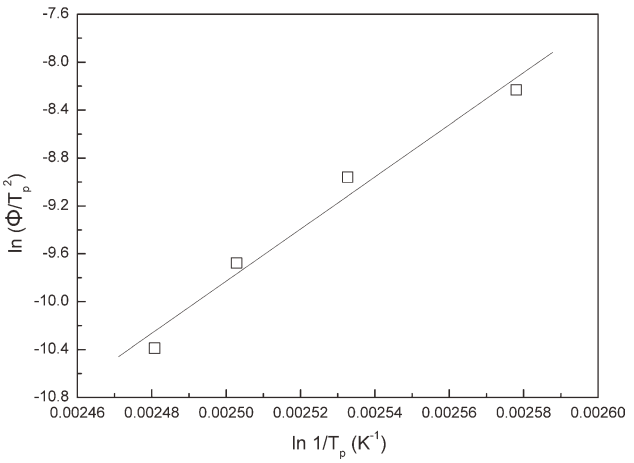

Figure 9 Nonisothermal crystallization kinetic curve of $\ln(\Phi/T_p^2)$ versus $\ln(1/T_p)$ according to the Kissinger method.

rate needed to be used to obtain a higher degree of crystallinity at a defined crystallization time. The values of α were almost the same for each sample.

When calculating the crystallization activation energy (see Fig. 9) using Kissinger method, we observed a good linearity, and the crystallization activation energy data of all of the β-nucleated PP/PTT samples are listed in Table V. It can be seen that the activation energy of the formation of β-crystal PP was larger than that of the formation of α-crystal PP. With the addition of PTT, the crystallization activation energy of β-nucleated PP increased. This may have been due to the fact that the solid PTT phase exhibited some heterogeneous nucleation effects on PP during its crystallization process, and it needed a lower crystallization activation energy for the PP phase to form the crystals. When SEP or PP-*g*-MA was added to the β-nucleated PP/PTT blends, the crystallization activation energy further increased and was close to that of the β-nucleated PP; this suggested that SEP and PP-*g*-MA in the PP matrix disturbed the crystallization process of PP and counteracted the promotion effect of the PTT phase.

CONCLUSIONS

The β-nucleated PP was incompatible with PTT, and the addition of the two compatibilizers decreased the interfacial tension between the β-nucleated PP and PTT. This led to improved dispersion and strengthened interfacial bonding in the blends. PP-*g*-MA had a better compatibilization effect. All of the researched β-nucleated PP/PTT blends contained β crystals of PP, and the compatibilizers exhibited a synergistic effect with a β-nucleating agent to further increase the β-crystal content. Nonisothermal kinetic analysis indicated that Mo's method satisfactorily described the nonisothermal crystallization behavior of the β-nucleated PP/PTT blends, and the Avrami method could only appropriately describe the early stage of crystallization, whereas the Ozawa method failed to have the same effect.

References

1. Varga, J. J Macromol Sci Phys 2002, 41, 1121.
2. Luo, F.; Geng, C. Z.; Wang, K.; Deng, H.; Chen, F.; Fu, Q. Macromolecules 2009, 42, 9325.
3. Chen, Y. H.; Zhong, G. J.; Wang, Y.; Li, Z. M.; Li, L. B. Macromolecules 2009, 42, 4343.
4. Zhu, H.; Monrabal, B.; Han, C. C.; Wang, D. Macromolecules 2008, 41, 826.
5. Menyhárd, A.; Varga. J.; Molnár, G. J Therm Anal Calorim 2006, 83, 625.
6. Moitzi, J.; Skalicky, P. Polymer 1993, 34, 3168.
7. Meille, S. V.; Ferro, D. R.; Bruckner, S.; Lovinger, A. J. Macromolecules 1994, 27, 2615.
8. Feng, M.; Gong, F. L.; Zhao, C. G.; Chen, G. M.; Zhang, S. M. J Polym Sci Part B: Polym Phys 2004, 42, 3428.
9. Varga, J. J Therm Anal 1989, 35, 1891.
10. Menyhárd, A.; Varga, J. Eur Polym J 2006, 42, 3257.
11. Yang, Z. G.; Chen, C. Y.; Liang, D. W.; Zhang, Z. S.; Mai, K. C. Polym Int 2009, 58, 1366.
12. Yang, Z. G.; Zhang, Z. S.; Tao, Y. J.; Mai, K. C. Eur Polym J 2008, 44, 3754.
13. Yang, Z. G.; Zhang, Z. S.; Tao, Y. J.; Mai, K. C. J Appl Polym Sci 2009, 112, 1.
14. Menyhárd, A.; Varga, J.; Liber, A.; Belina, G. Eur Polym J 2005, 41, 669.
15. Yang, Z. G.; Mai, K. C. Thermochim Acta 2010, 511, 152.
16. Wang, Y. J.; Run, M. T. J Polym Res 2009, 16, 725.
17. Jafari, S. H.; Yavari, A.; Asadinezhad, A. Polymer 2005, 46, 5082.
18. Huang, J. M. J Appl Polym Sci 2003, 88, 2247.
19. Turner-Jones, A.; Aizlewood, J.; Beckett, D. Macromol Chem Phys 1964, 75, 134.
20. Wu, S. H. J Polym Sci Part C: Polym Symp 1971, 34, 19.
21. Herrero, C. H.; Acosta, J. L. Polym J 1994, 26, 786.
22. Caze, C.; Devaux, E.; Crespy, A.; Cavrot, J. P. Polymer 1997, 38, 497.
23. Ozawa, T. Polymer 1971, 12, 150.
24. Ozawa, T. J Therm Anal 1970, 2, 301.
25. Liu, S. Y.; Yu, Y. N.; Cui, Y.; Zhang, H. F.; Mo, Z. S. J Appl Polym Sci 1998 70, 2371.
26. Liu, T. X.; Mo, Z. S.; Wang, S. G.; Zhang, H. F. Polym Eng Sci 1997, 37, 568.
27. Kissinger, H. E. Res J Natl Bureau Stand 1956, 57, 63.
28. Strŏm, G.; Fredriksson, M.; Stenius, P. J Colloid Interface Sci 1987, 119, 352.
29. Erbil, H. Y. Handbook of Surface and Colloid Chemistry; Birdi, K. S., Ed.; Wiley: Boca Raton, 1997; Chapter 9. pp 265-312.
30. Koide, S.; Yazawa, K.; Asakawa, N.; Inoue, Y. J Mater Chem 2007, 17, 582.